

# Topographic characterization and electrostatic response of *M*-DNA studied by atomic force microscopy

F Moreno-Herrero<sup>1,3</sup>, P Herrero<sup>2</sup>, F Moreno<sup>2</sup>, J Colchero<sup>1</sup>,  
C Gómez-Navarro<sup>1</sup>, J Gómez-Herrero<sup>1</sup> and A M Baró<sup>1</sup>

<sup>1</sup> Laboratorio de Nuevas Microscopías, Departamento de Física de la Materia Condensada, Universidad Autónoma de Madrid, E-28049, Madrid, Spain

<sup>2</sup> Departamento de Bioquímica y Biología Molecular, Instituto Universitario de Biotecnología de Asturias, Universidad de Oviedo, 33006, Oviedo, Spain

E-mail: fernando.moreno@uam.es

Received 16 September 2002, in final form 19 November 2002

Published 10 January 2003

Online at [stacks.iop.org/Nano/14/128](http://stacks.iop.org/Nano/14/128)

## Abstract

Modified DNA species have attracted the interest of the scientific community in the last years in a search for an appropriate molecular wire for the incoming nanotechnology. *M*-DNA, a complex of DNA with divalent metallic ions, is one of the candidates for a molecular wire. In this paper we describe the procedure to fabricate *M*-DNA using NiCl<sub>2</sub> and CoCl<sub>2</sub>, and a simple test to check the production of the modified biomolecule. We present atomic force microscope (AFM) images of nickel and cobalt *M*-DNA. Our results show that the DNA modified with these metal ions suffers a fivefold reduction in length and an increment of almost one order of magnitude in height as compared to the length and height of regular *B*-DNA. This type of condensation of the DNA is fully reversible upon the addition of EDTA. AFM images of reversed *M*-DNA show no differences from regular *B*-DNA. Two types of electrostatic experiment performed on this modified molecule show no evidence for metallic or semiconductor behaviour.

(Some figures in this article are in colour only in the electronic version)

## 1. Introduction

In recent years, the scientific community has focused on the search for an appropriate molecular wire for the incoming nanotechnology. Among other molecules, DNA has experienced intense research trying to characterize its electrical properties [1–8]. To date, the electric behaviour of *B*-DNA is still under debate. Metallic engineered DNA, *M*-DNA, has also been proposed as a molecular wire [9, 10]. *M*-DNA has attracted interest because some unusual electrical properties have been reported [9, 10]. However, to date the effect of the metal ions on the structure of the regular *B*-DNA is not clear and no surface characterization has been reported. If future experiments confirm the possibilities of this modified molecule in the field of nanotechnology, topological characterization of

these molecules should be of great importance.

*M*-DNA has been described as a complex of *B*-DNA with the divalent metal ions Co<sup>2+</sup>, Ni<sup>2+</sup> and Zn<sup>2+</sup>. Present knowledge concerning *M*-DNA properties mainly derives from studies with bacterial and synthetic DNAs [11]. These studies have characterized, in different detail, several properties.

- (i) *M*-DNA does not bind ethidium bromide, thus a 'fluorescence assay' in the presence of ethidium bromide can be used to monitor *M*-DNA formation.
- (ii) The mobility of *M*-DNA in agarose gels has been postulated to be similar to that of *B*-DNA; this observation suggests that metal ions do not cause condensation of the DNA.
- (iii) It was suggested that the imino protons of T and G were replaced in *M*-DNA by the metal ion during the *B*-DNA to *M*-DNA transition.

<sup>3</sup> Author to whom any correspondence should be addressed.

We have used atomic force microscopy (AFM), also called scanning force microscopy (SFM), to characterize the surface of the metal modified DNA. The AFM was invented in 1986 [12]. Since then, it has become a routine technique of surface characterization. The technique has experienced an enormous growth, specially in the field of biophysics, and in particular in DNA imaging [13–23].

In this paper we describe a simple protocol to produce *M*-DNA. Cobalt and nickel modified DNA results in a reduction of its longitudinal dimension as well as an increment of the molecular height. We deduce that the presence of these metal ions in the DNA condenses the molecule. Release of the DNA molecules from the *M*-DNA state was achieved experimentally by removal of the divalent cations through EDTA chelation.

In order to investigate whether the electrical transport properties of DNA are affected by the intercalation of metal ions we have used AFM. Firstly, we have carried out a topographic characterization of the *M*-DNA molecules and secondly, we have used AFM to study the electrical properties of the modified DNA molecules. This has been accomplished by performing two types of electrostatic experiment on *M*-DNA following [8, 24]. These two experiments show no evidence for molecular wire behaviour of *M*-DNA as reported on non-modified DNA [8].

## 2. Materials and methods

### 2.1. *M*-DNA sample preparation

To generate DNA linear fragments of different lengths, the pUC18 and YEp13 plasmids were linearized at unique *Bam*HI sites. Two linear fragments of 2690 bp and 10 667 bp were obtained. These DNA fragments were used to prepare DNA modified molecules with the divalent ions Ni<sup>2+</sup> and Co<sup>2+</sup>. The DNA fragments were dissolved in 90 mM tris borate buffer, pH 8.5, at a concentration of approximately 0.1 mg ml<sup>-1</sup>. 5  $\mu$ l DNA aliquots were added to 20  $\mu$ l of a buffer containing 90 mM tris borate and 10 mM NiCl<sub>2</sub> or 1 mM CoCl<sub>2</sub>, pH 8.5. The pH of the resulting assay mixture was maintained at approximately 8.5 with 1 M KOH. Typical reaction times were 40–45 min at room temperature.

Because the *M*-DNA does not bind ethidium bromide [9], *M*-DNA formation was followed by agarose electrophoresis measuring the fluorescence of intercalated ethidium bromide. To localize *M*-DNA in the agarose electrophoresis the DNA samples were labelled with [ $\alpha$ -<sup>32</sup>P]dCTP by filling in the protruding 5' ends in the presence of Klenow fragments.

### 2.2. AFM imaging

AFM images were obtained with a commercial AFM [25]. We have used non-contact dynamic SFM for all the images shown. We used soft cantilevers of nominal force constant 1 N m<sup>-1</sup>, resonance frequency 75–80 kHz and tip radius 15–20 nm [26]. The cantilever is oscillated at its resonance frequency. The amplitude and the relative phase of the oscillation are measured through the normal force signal. The feedback is performed on the amplitude signal channel. In this manner tip–sample distance is kept constant. The tip is at, typically, a few nanometres above the surface and the amplitude of the oscillation at which the images are taken is about 25 nm. For more details see [27, 28].

### 2.3. AFM sample preparation

Mica is an appropriate substrate for imaging biomolecules with AFM [29–31]. Mica exposes a negatively charged surface when cleaved, therefore, divalent cations like Zn<sup>2+</sup> or Mg<sup>2+</sup> are employed to adsorb negatively charged molecules like DNA [17]. We have found that the absence of this divalent ion inhibits the adsorption of the molecules to the mica. The standard DNA sample preparation protocol for AFM consists of a final mixture of 1–10 mM MgCl<sub>2</sub> and 10–100 ng of DNA diluted in tris EDTA buffer placed on a freshly cleaved mica disc and extensively washed with double-deionized ultrapure water. Finally, the sample is dried with a gentle stream of air or dry nitrogen. Using an AFM, DNA molecules so prepared can be easily imaged [21, 32]. For *M*-DNA, no extra addition of divalent cations was necessary. 5  $\mu$ l of the *M*-DNA reaction were placed on a mica disc and then we followed the washing and drying part as described above. The concentration of *M*-DNA molecules was checked by AFM inspection.

For the first electrostatic experiment on *M*-DNA, a 30 nm thick film of gold was evaporated on the samples partially covering the molecules as described in [1]. The electrostatic method employed here is described in detail in [8]. For the second electrostatic experiment no additional evaporation was needed. AFM tips employed in the electrostatic experiments were covered with 20 nm of titanium and 20 nm of gold.

## 3. Results and discussion

Nickel and cobalt *M*-DNA samples were prepared as described in section 2. It is known that ethidium bromide (EtBr) does not bind *M*-DNA [9]. We have used this property of *M*-DNA to design a 'fluorescence assay', in the presence of EtBr, to monitor *M*-DNA formation. 5  $\mu$ l DNA aliquots were added to 20  $\mu$ l of a buffer containing 90 mM tris borate and from 0.1 to 100 mM NiCl<sub>2</sub> or from 10  $\mu$ M to 50 mM CoCl<sub>2</sub>, pH 8.5, using the assay conditions described above. After 45 min incubation at room temperature the samples were subject to electrophoresis in a horizontal 0.8% agarose gel at 10 V cm<sup>-1</sup> of gel for 45 min in 0.5  $\times$  TB (45 mM tris borate, pH 8.5) containing 5  $\mu$ g EtBr. The minimum cation concentration that allows no binding of EtBr to DNA was selected for Ni<sup>2+</sup> (10 mM) and Co<sup>2+</sup> (1 mM) ions (figure 1(A)). As can be seen in figure 1 (lanes 2 and 3), the fluorescence of the modified DNA disappears because *M*-DNA does not bind ethidium bromide. The unmodified *B*-DNA remains fluorescent (lane 1). This simple and easy test was used routinely to check the production of *M*-DNA.

In order to know the exact position of the *M*-DNA in the gel, the DNA was radioactively labelled with [ $\alpha$ -<sup>32</sup>P]dCTP by filling in the protruding 5' ends in the presence of Klenow fragment DNA polymerase. After agarose gel electrophoresis of the DNA samples, gels were autoradiographed at –70 °C with an intensifying screen (figure 1(B)). One interesting find is that the *M*-DNA does not enter the gel matrix. This can be explained in two manners: either *M*-DNA does not have any type of net charge and in consequence does not run into the agarose gel or the modified DNA cannot enter the gel because of sterical factors. The pore size of a 0.8% agarose gel is about 50 nm [33]. If the modified DNA does not enter the

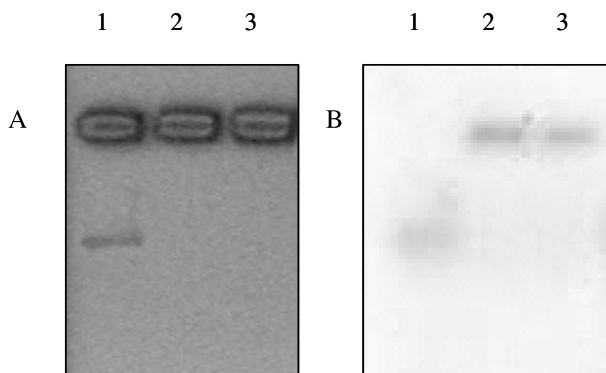


**Figure 1.** Radioactive experiment which shows the formation of metal modified DNA. (A) The fluorescence of the ethidium bromide as the gel is illuminated with ultraviolet light. Lane 1 is the unmodified DNA and in lanes 2 and 3 are the Co and Ni modified DNA respectively. The DNA employed was previously labelled with [ $\alpha$ - $^{32}$ P]dCTP. The radiograph is shown in part B of the figure. Lanes 2 and 3 are now present showing that the modified DNA does not enter the agarose gel.

gel because it cannot fit the pore, it must have an structure of tens of nanometres. This result is in contradiction with the mobility in agarose gels of *M*-DNA reported before [9]. To know more about the physical appearance of the *M*-DNA, we have used the ability of the AFM to image insulating samples at the nanometre scale.

*M*-DNA samples for AFM experiments were bound to a mica surface for imaging. Interestingly, it was not necessary to add any extra ions to the *M*-DNA samples to assist binding to the mica substrate. This indicates that the modified DNA has some kind of charge. We should, then, discard the hypothesis of the lack of charge as the reason why the *M*-DNA does not enter an agarose gel. We think that the excess of divalent ions ( $\text{Ni}^{2+}$  or  $\text{Co}^{2+}$ ) binds to the surface and charges it. The positively charged mica is then appropriate for binding the *M*-DNA. It has been reported that the use of other divalent ions than  $\text{Mg}^{2+}$  also promotes adhesion of DNA to the mica surface [34, 35].

Atomic force microscopy images of  $\text{Ni}^{2+}$  and  $\text{Co}^{2+}$  *M*-DNA are shown in figure 2. A set of images at different magnifications is shown. No major differences between  $\text{Ni}^{2+}$  or  $\text{Co}^{2+}$  modified species of DNA were found from the AFM images. Figure 2(A) is a  $5\ \mu\text{m} \times 5\ \mu\text{m}$  image where *M*-DNA molecules can be seen. The *B*-DNA, in this case, is a linearized plasmid of 10 667 bp ( $3.6\ \mu\text{m}$ ). One characteristic of the *M*-DNA molecules is that they are much shorter than the regular *B*-DNA. In figure 2(A) the longest molecule found has a length of 600–700 nm. There is a typical fivefold shortening in the length. Another interesting feature of the sample is the o-ring shapes detected everywhere. This can be explained because the Yep13 plasmid was linearized with *Bam*HI. This restriction enzyme leaves a four-base overhang. During the *M*-DNA production process the DNA could be annealed forming a circular shape. The interesting feature of the DNA shortening during the *B*-DNA to *M*-DNA transition is clearly visible in figure 2(B) (a  $3\ \mu\text{m} \times 3\ \mu\text{m}$  image) and figures 2(C) and (D) (details of  $1\ \mu\text{m}$  size).

The other interesting feature is the height of the *M*-DNA. *M*-DNA molecules appear higher than *B*-DNA molecules.

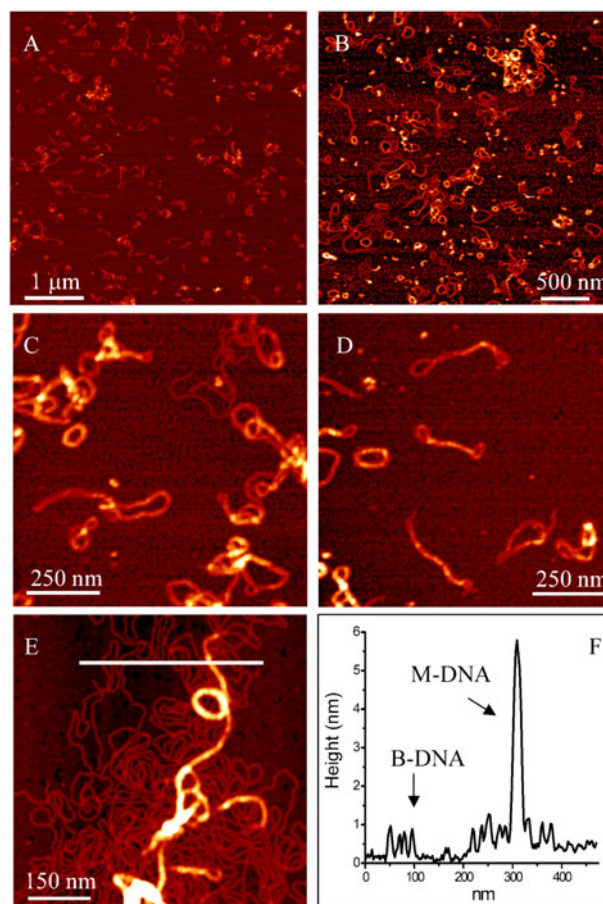


**Figure 2.** AFM images of *M*-DNA. A set of images at different magnifications of *M*-DNA is shown in (A), (B), (C) and (D). DNA of 10 667 bp ( $3.6\ \mu\text{m}$ ) was employed in this experiment. The effect of the shortening of the molecules is clear. (F) is a height profile taken along the line marked in (E), where both structures, *M*-DNA and *B*-DNA, coexist in this image. The different heights of the DNA in the *M*-form and in the *B*-form are clear. *M*-DNA experiences a reduction in length and a increase in height. *M*-DNA height is up to one order of magnitude bigger than the height of the regular DNA.

Figure 2(E) shows a  $2\ \mu\text{m} \times 2\ \mu\text{m}$  image of  $\text{Ni}^{2+}$ -*M*-DNA. In this case, most of the DNA remains in the *B*-DNA appearance. This type of sample, where both appearances coexist, is quite common but in all cases these molecules were never detected in the fluorescence assay used to monitor the *M*-DNA formation. This proves that they are somehow modified. Figure 2(F) shows a profile of figure 2(E). The difference in height between *M*-DNA and *B*-DNA is clear. The measured height of the *M*-DNA is between 5 and 7 nm, close to one order of magnitude greater than the height of regular adsorbed DNA imaged with AFM [36]. *M*-DNA bundles of 20–30 nm height such as the one described in [10] were never found in our AFM samples.

To test the reversibility of the *M*-DNA formation process an additional experiment summarized in figure 3 was carried out.  $\text{Co}^{2+}$  and  $\text{Ni}^{2+}$  *M*-DNA samples were prepared and the *M*-DNA formation was monitored by the ‘fluorescence assay’, following the protocol described above (figure 3(A)). In order to analyse the reversibility of the *M*-DNA reaction,  $5\ \mu\text{l}$  of  $\text{Co}^{2+}$  and  $\text{Ni}^{2+}$  *M*-DNA samples were added to  $20\ \mu\text{l}$  of a buffer containing 90 mM tris borate and 150 mM EDTA, pH 8.5.

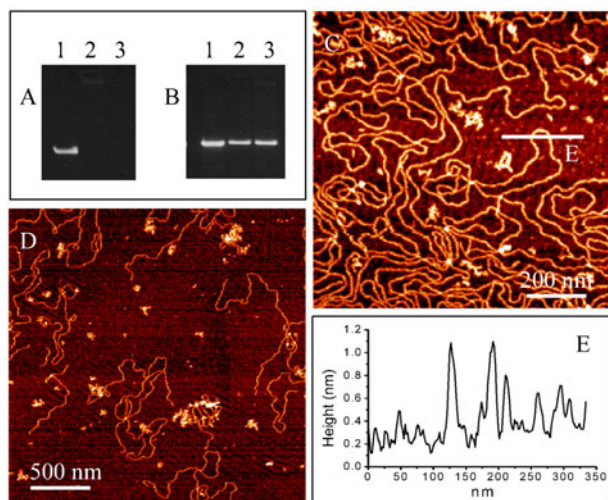


**Figure 3.** Experiment showing the reversibility of the *M*-DNA formation upon the addition of EDTA. (A) is the agarose gel showing the *M*-DNA formation. Bands in lanes 2 and 3 are not visible. (B) is the same experiment but after EDTA has been added to the *M*-DNA sample. In this case bands in lanes 2 and 3 appear visible, consistent with the reversibility of the process of *M*-DNA formation. This DNA is imaged with AFM as shown in (C) and (D). In (E) a height profile of the reversed *M*-DNA is shown. The typical height of DNA (0.8 nm) is now achieved.

After 45 min incubation at room temperature the samples were subjected to electrophoresis in a horizontal 0.8% agarose gel at  $10 \text{ V cm}^{-1}$  of gel for 45 min in  $0.5 \times \text{TBE}$  (45 mM tris borate, 1 mM EDTA, pH 8.5) containing  $5 \mu\text{g EtBr}$ . Figure 3(B) shows that the  $\text{Co}^{2+}$  and  $\text{Ni}^{2+}$ -*M*-DNA samples recovers the mobility and the capacity to bind EtBr of *B*-DNA in the presence of EDTA. Thus, the process of the *M*-DNA formation is apparently reversible by the ‘fluorescence assay’ analysis.

The EDTA-*M*-DNA was also inspected by AFM. The AFM sample preparation was performed as usual for *B*-DNA. In this way the addition of divalent ions was essential to assist binding to the mica. Figures 3(C) and (D) show two AFM images at different magnifications showing DNA molecules with the typical appearance of *B*-DNA. The height of these molecules was found to be  $0.8 \pm 0.2 \text{ nm}$  in complete agreement with the height of regular DNA [36]. Our results demonstrate that the process of *M*-DNA formation is reversible and the condensation phenomenon can be controlled.

The electrostatic experiments performed on *M*-DNA are shown in both figures 4 and 5. The electrostatic methods used are described in [8, 24]. The basic idea of the experiment shown in figure 4 is that metallic or semiconductor molecules appear higher and wider when a voltage is applied between the tip and the gold electrode. *M*-DNA molecules are easy to identify because of their characteristic twisted appearance. Figure 4(B) is the same area but a bias voltage of 8 volts is applied between tip and sample. Due to the electrostatic interaction between the tip and the sample the gold electrode is poorly resolved as expected [8, 37], but the modified DNA molecule remain the same.

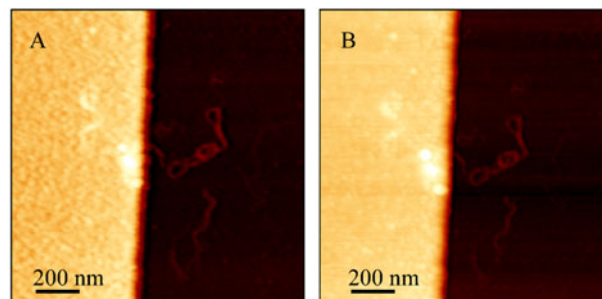


**Figure 4.** Electrostatic experiment on *M*-DNA. Molecules can be clearly seen partially covered by a 30 nm gold film. In (A), no bias voltage is applied between the tip and the gold electrode. In (B), a bias voltage of 8 volts is applied. While the contour of the gold grains gets diffuse due to the electrostatic interaction, the appearance of the *M*-DNA molecules remains the same as in (A).

We have further confirmed our result by carrying out a final experiment without any electrode. This experiment is similar to the one performed on *B*-DNA and carbon nanotubes explained in [24]. This experiment provides more quantitative information related to the electrostatic interaction between the tip and the *M*-DNA molecule. This experiment is described in figure 5. Figure 5(B) shows an AFM topographic image of DNA molecules in *B*- and *M*-forms. After this topographic image, the tip is lifted 75 nm above the mica substrate while oscillating at the free resonance frequency of the cantilever. A bias voltage of 6 volts is then applied to the metal covered tip. As the tip approaches the surface while scanning over the molecules a monotonic decrease of the resonance frequency  $\Delta\omega$  is observed because of the electrostatic force produced by the polarization of the insulating substrate. Figure 5(C) shows a frequency shift profile taken along the black line in figure 5(B). The profile was taken with the tip (bias 6 volts) positioned at 15 nm above the sample. No signal above our noise level is detected when the tip is over the *M*-DNA molecule, showing that the dielectric constant of the *M*-DNA molecules is similar to the one of the substrate. This result shows that *M*-DNA molecules behave as insulators when adsorbed on a mica substrate, confirming our previous findings. The absence of any contrast in electrostatic interaction above the offset level caused by the substrate also indicates that this electrostatic interaction cannot affect the measured height of the *M*-DNA molecules.

#### 4. Conclusion

We have presented one of the first AFM measurements of metallic engineered DNA samples (*M*-DNA). We have shown an easy and quick method to obtain *M*-DNA and a way to test the production through a ‘fluorescence assay’ in the presence of ethidium bromide. Our results demonstrate that *M*-DNA cannot enter an 0.8% agarose gel because the size of the modified structures is bigger than the pore size. AFM measurements on *M*-DNA samples shows a fivefold shortening in the length of the DNA as well as an increment in the height of almost one order of magnitude. This kind of condensation could be important to explain previous results obtained on this kind of molecule regarding the electrical properties of the modified DNA. We have also used the AFM to

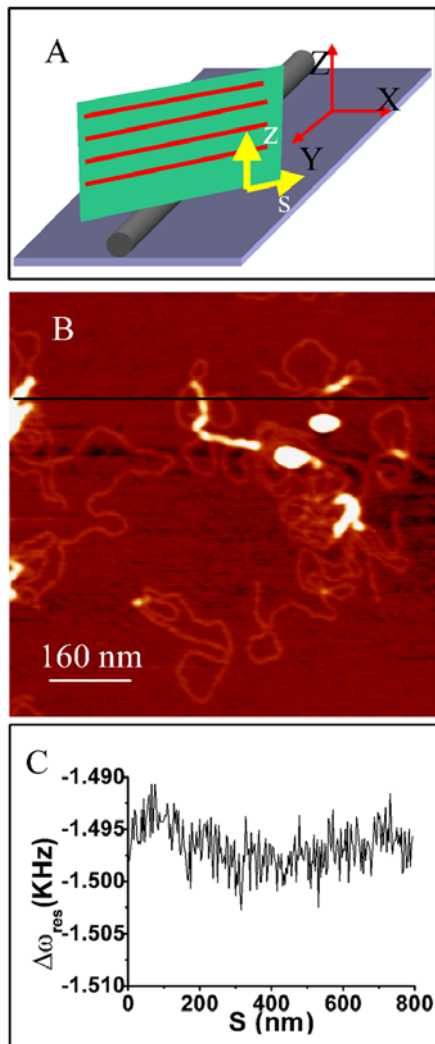


**Figure 5.** (A) Scheme of the contactless experiment performed on a *M*-DNA. Frequency shift profiles are taken at different tip-sample distances over the line marked in (B). The one shown in (C) was obtained at 15 nm above the substrate when a bias voltage of 6 volts was applied to the metal AFM tip. As can be seen no contrast above the noise level is observed, indicating that the *M*-DNA molecule behaves as an insulator.

prove that the reaction of the *M*-DNA formation is reversible upon the addition of EDTA. The AFM images demonstrate that the *M*-DNA molecules treated with EDTA recover their nominal length and height typical for the DNA in *B*-form. The electrostatic experiments performed on *M*-DNA molecules show no evidence for molecular wire behaviour since no topographic modification on the molecules is observed when a bias voltage is applied between the metallized tip and the electrode that covers them. In addition, no change in the resonance frequency of the cantilever is detected when the biased tip passes over the *M*-DNA molecules, confirming the insulating nature of the *M*-DNA.

### Acknowledgments

FM-H is supported by a fellowship from the Comunidad Autónoma de Madrid. We acknowledge support from

Ministerio de Educacion y Cultura through the DGESIC projects BFM2001-0150 and BMC2001-1690-C0202.

### References

- [1] de Pablo P J, Moreno-Herrero F, Colchero J, Gómez-Herrero J, Herrero P, Baró A M, Ordejon P, Soler J M and Artacho E 2000 *Phys. Rev. Lett.* **85** 4992–5
- [2] Porath D, Bezryadin A, de Vries S and Dekker C 2000 *Nature* **403** 635–8
- [3] Conwell E M and Rakhmanova S V 2000 *Proc. Natl Acad. Sci. USA* **97** 4556–60
- [4] Cai L, Tabata H and Kaway T 2000 *Appl. Phys. Lett.* **77** 3105–6
- [5] Kasumov A Y, Kociak M, Gueron S, Reulet B, Volkov V T, Klinov D V and Bouchiat H 2001 *Science* **291** 280–2
- [6] Giese B, Amaudrut J, Kohler A K, Spormann M and Wessely S 2001 *Nature* **412** 318–20
- [7] Storm A J, van Noort J, de Vries S and Dekker C 2001 *Appl. Phys. Lett.* **79** 3881–3
- [8] Gómez-Navarro C, Moreno-Herrero F, de Pablo P J, Colchero J, Gómez-Herrero J and Baró A M 2002 *Proc. Natl Acad. Sci. USA* **99** 8484–7
- [9] Aich P, Labiuk S L, Tari L W, Delbaere L J, Roesler W J, Falk K J, Steer R P and Lee J S 1999 *J. Mol. Biol.* **294** 477–85
- [10] Rakitin A, Aich P, Papadopoulos C, Kobzar Y, Vedenev A S, Lee J S and Xu J M 2001 *Phys. Rev. Lett.* **86** 3670–3
- [11] Lee J S, Latimer L J and Reid R S 1993 *Biochem. Cell. Biol.* **71** 162–8
- [12] Binnig G, Quate C F and Gerber C 1986 *Phys. Rev. Lett.* **56** 930–3
- [13] Hansma H G, Sinsheimer R L, Li M Q and Hansma P K 1992 *Nucleic Acids Res.* **20** 3585–90
- [14] Bustamante C, Vesenka J, Tang C L, Rees W, Guthold M and Keller R 1992 *Biochemistry* **31** 22–6
- [15] Shaiu W L, Larson D D, Vesenka J and Henderson E 1993 *Nucleic Acids Res.* **21** 99–103
- [16] Lyubchenko Y, Shlyakhtenko L, Harrington R, Oden P and Lindsay S 1993 *Proc. Natl Acad. Sci. USA* **90** 2137–40
- [17] Thomson N H, Kasas S, Smith B, Hansma H G and Hansma P K 1996 *Langmuir* **12** 5905–8
- [18] Hansma H G, Revenko I, Kim K and Laney D E 1996 *Nucleic Acids Res.* **24** 713–20
- [19] Lyubchenko Y L, Shlyakhtenko L S, Aki T and Adhya S 1997 *Nucleic Acids Res.* **25** 873–6
- [20] Maeda Y, Matsumoto T and Kaway T 1999 *Appl. Surf. Sci.* **140** 400–5
- [21] Moreno-Herrero F, Herrero P, Colchero J, Baró A M and Moreno F 1999 *FEBS Lett.* **459** 427–32
- [22] Ye J Y, Umemura K, Ishikawa M and Kuroda R 2000 *Anal. Biochem.* **281** 21–5
- [23] Hansma H G 2001 *Annu. Rev. Phys. Chem.* **52** 71–92
- [24] Gómez-Navarro C, de Pablo P J, Moreno-Herrero F, Horcas I, Fernandez-Sánchez R, Colchero J, Gómez-Herrero J and Baró A M 2002 *Nanotechnology* **13** 1–4
- [25] Nanotec Electronica S L, Madrid, www.nanotec.es
- [26] Olympus Optical Co., Ltd
- [27] de Pablo P J, Colchero J, Luna M, Gómez-Herrero J and Baró A M 2000 *Phys. Rev. B* **61** 14179–83
- [28] Moreno-Herrero F, de Pablo P J, Colchero J, Gómez-Herrero J and Baró A M 2000 *Surf. Sci.* **453** 152–8
- [29] Bustamante C, Erie D A and Keller D 1994 *Curr. Opin. Struct. Biol.* **4** 750–60
- [30] Bustamante C, Rivetti C and Keller D J 1997 *Curr. Opin. Struct. Biol.* **7** 709–16
- [31] Engel A, Schoenenberger C A and Muller D J 1997 *Curr. Opin. Struct. Biol.* **7** 279–84
- [32] Moreno-Herrero F, Herrero P, Colchero J, Baró A M and Moreno F 2001 *Biochem. Biophys. Res. Commun.* **280** 151–7

- [33] Rebecca H L, Altreuter D H and Gentile F T 1995 *Biotechnol. Bioeng.* **50** 365–73
- [34] Vesenka J, Guthold M, Tang C L, Keller D, Delaine E and Bustamante C 1992 *Ultramicroscopy* **42–44** 1243–9
- [35] Hansma H G, Bezanilla M, Zenhausern F, Adrian M and Sinsheimer R L 1993 *Nucleic Acids Res.* **21** 505–12
- [36] Moreno-Herrero F, Colchero J and Baró A M *Ultramicroscopy*
- [37] de Pablo P J, Gómez-Navarro C, Gil A, Colchero J, Martínez M T, Benito A M, Maser W K, Gómez-Herrero J and Baró A M 2001 *Appl. Phys. Lett.* **79** 2979–81